

pubs.acs.org/Macromolecules Article

ToF-SIMS Depth Profiling to Measure Nanoparticle and Polymer Diffusion in Polymer Melts

Kaitlin Wang, Russell J. Composto, and Karen I. Winey*



ACCESS

Metrics & More

Article Recommendations

Supporting Information

ACCESS

Article Recommendations

Supporting Information

Distance (µm)

ABSTRACT: We apply time-of-flight secondary ion mass spectroscopy (ToF-SIMS) and cross-sectioned trilayer samples to separately measure nanoparticle (NP) and polymer diffusion on micrometer length scales in polymer melts. We fabricate polymer/diffusing medium/polymer trilayer samples and measure the cross section to extract the NP or deuterated polymer distribution in 3D using ToF-SIMS. After correcting the data for sample tilt, deconvoluting the beam resolution, and integrating the data to extract 1D concentration profiles, we fit the data to extract the diffusion coefficient. These results from cross-sectional ToF-SIMS are in excellent agreement with earlier studies using well-established ion beam methods. This work establishes ToF-SIMS as a reliable tool for measuring NP and polymer diffusion coefficients and opens the door to investigating diffusion in more complex polymer systems and across longer time and length scales.

■ INTRODUCTION

Polymer nanocomposites (PNCs) are valued for their tunable and enhanced properties that lead to applications in industrial rubbers, gas separation membranes, and dielectric materials. Their properties depend on the composition and PNC morphology as well as the mobility of the polymer and nanoparticles in the PNC. Nanoparticle (NP) diffusion plays an important role during PNC processing and the resulting PNC structure and properties. For example, NP diffusion is essential for PNC applications in self-healing materials and drug delivery. Similarly, polymer diffusion is foundational to understanding polymer melts including homopolymers, copolymers, binary polymer blends, and PNCs. 6–11

Current methods for measuring NP and polymer diffusion are limited on their time and length scales, the accessible geometries, and the availability of the experimental tools. ^{12,13} Previous NP diffusion studies in polymer melts have used dynamic light scattering (DLS), X-ray photon correlation spectroscopy (XPCS), ^{14,15} single particle tracking (SPT), ¹⁶ and Rutherford backscattering spectrometry (RBS). ^{17,18} DLS is an affordable and accessible method that probes diffusion in liquid environments through fitting the intensity correlation function to determine reflecting translational Fickian diffu-

sion sion sion sion same provides an ensemble measurement of the diffusion coefficient. Using the same fundamental principles, XPCS requires a synchrotron to probe NP diffusion. SPT instruments are fairly accessible and directly measure mean-squared displacement of particles to probe diffusion and has been used to capture heterogeneous diffusion. Because DLS, XPCS, and SPT require both low $T_{\rm g}$ ($T_{\rm g} < T_{\rm room}$) matrices or liquid environments and very dilute systems, these methods are unable to explore many industrially relevant conditions of PNCs with crowded, polydisperse, strongly attractive, or nonspherical nanoparticles. On the smallest length scales (nm), neutron reflectivity (NR) has been used to probe diffusion of soft nanoparticles and polymer tracer diffusion in polymer melts. Polymer diffusion studies have also used elastic recoil detection (ERD), formerly known as forward

Received: January 6, 2023 Revised: February 27, 2023 Published: March 16, 2023





recoil spectroscopy (FRES), to determine self-diffusion coefficients, 9,23 but similar to RBS, ERD is becoming less accessible and probes a limited length scale.

RBS and ERD, which use MeV incident ions, are the closest analogues to our time-of-flight secondary ion mass spectroscopy (ToF-SIMS) method and are well-established for measuring polymer and NP diffusion. 17,24-26 Similar to ToF-SIMS, RBS determines the NP diffusion coefficient independent by measuring the depth profile of the NP and then fitting the profile with a diffusion model. In Griffin's work, the NP concentration of a bilayer sample comprising a PNC film (\sim 100–200 nm) on a thick polymer layer (\sim 10 μ m) was measured using RBS after ex situ annealing for 0-30 min at 180 °C. 17 RBS is limited to measuring NP diffusion in polymer melts with $T_{\rm g} > T_{\rm room}$ to depths of $\sim 1~\mu{\rm m}$ and has limited chemical sensitivity. For polymer diffusion, ERD was similarly applied to depth-profile deuterated polymer/nondeuterated polymer bilayers due to its ability to measure deuterium concentration profiles.^{6,23,27–30} These 1-D concentration profiles are fit with Fickian diffusion equations to find the NP and polymer diffusion coefficients. Because of limitations on NP and polymer diffusion measurements including detection limits or specialized materials (deuteration or fluorescence), and increasingly limited access to RBS and ERD, we developed a method applying ToF-SIMS, an increasingly available experimental tool. Our cross-sectional ToF-SIMS method significantly expands accessible compositions and diffusion length scales (0.5-200 μ m) and increases the feasibility of diffusion studies in polymer systems across an exceptionally broad range of diffusion coefficients ($\sim 10^{-15}$ to $10^{-6} \text{ cm}^2/\text{s}$).

ToF-SIMS operates by accelerating a focused beam of keV ions of a specified energy toward a sample to eject secondary ions to a time-of-flight detector, which measures the mass and charge of the ejected species. Mass-to-charge ratios (m/q)are characteristic of the species (atomic or clusters) to provide compositional information on the sample, including distinguishing isotopes, e.g., hydrogen and deuterium.³² ToF-SIMS is traditionally used to measure composition as a function of depth from the sample surface. In contrast to this traditional sample orientation, compositional variations deeper within a sample can be expedited by scanning a cross section of the sample, as demonstrated in our method. As the primary beam sputters the sample, ToF-SIMS collects three-dimensional compositional data, providing 3D maps for each secondary ion detected with $<1 \mu m^2$ lateral resolution. ToF-SIMS is a wellestablished method for depth profiling inorganic systems, with more recent applications in polymer systems. 31,33 Cluster ion beams, with improved high mass sensitivity compared to primary ion sources, have been used successfully to depth profile polystyrene (PS) and polyvinylpyrrolidone (PVP) layers to depths of 15 μ m, with depth resolution comparable to ellipsometry (<10 nm).³⁴ Depth profiling in ToF-SIMS has also been applied to polymer-based cathode materials, for which dopant and ion concentration distributions determine conductive properties.³⁵ Primary ion beam ToF-SIMS is also capable of measuring filler distribution in polymer composites as Karar and Gupta accomplished in a carbon nanotube (CNT)-polyurethane composite on 100 μ m length scales.³⁶

Applying ToF-SIMS to polymer systems has known challenges, especially when using a primary ion source. With primary ion sources like our own, signal intensity in the high mass range is drastically lowered due to the high rate of

fragmentation.^{31,33} The destructive nature of SIMS and the yield-decreasing effects of charging on polymer samples make quantification difficult. ToF-SIMS data analysis is also complicated by the matrix effect, wherein ion yield is dependent on the atom's local environment. For example, surface oxidation causes high yield of secondary ions, skewing counts in the initial frames of collection.^{31,33} Depth profiling analysis is likewise complicated by ion beam mixing, reducing depth resolution.

Here, we demonstrate the capability of ToF-SIMS to measure NP and polymer diffusion in polymer melts by using trilayer samples, optimizing instrumental parameters, and developing a data analysis method to extract 1D NP or deuterated polymer concentration profiles. We determine the tracer NP diffusion coefficient in a silica/poly(2-vinylpyridine) (SiO₂/P2VP) PNC system. After varying annealing from 1 to 5 days, we can extract a concentration profile of the silica by scanning across an exposed cross section and determine a timeindependent diffusion coefficient (D_{NP}) from 10 vol % PNC films. We also measured the NP diffusion coefficient in P2VP as a function of NP concentration. We compare our NP diffusion coefficient with well-established RBS results and find excellent agreement, noting that our ToF-SIMS method accesses length scales an order of magnitude larger by performing laterally resolved depth profiling on a crosssectioned trilayer sample. In a second study, we determine the concentration profile of a deuterated polystyrene (dPS) tracer film diffusing into PS and compare the resulting diffusion coefficients with ERD studies find excellent agreement using the ToF-SIMS on cross-sectioned trilayers. Taken together, these two studies validate our ToF-SIMS method as a reliable method to measure NP and polymer diffusion, establishing it as a valuable tool to rejuvenate diffusion studies by expanding the range of accessible diffusion length scales to test current models, and investigate systems that were previously limited by compositional contrast or particle loading.

EXPERIMENTAL METHODS

Materials. Poly(2-vinylpyridine) (P2VP) (100 kg/mol, PDI 1.3, $R_{\sigma} = 7$ nm) was purchased from Polymer Source and used as-received. R_g° was determined at the National Institute of Standards and Technology (NIST) using small-angle neutron scattering (SANS) (Figure S1). Nissan-STL silica (SiO₂) nanoparticles ($R_{NP} = 26.1$ nm, PDI 1.19) were solvent-exchanged from methyl ethyl ketone (MEK) to methanol (MeOH) via crashing the particles out of MEK. Specifically, the MEK-NP solution was diluted with 50 vol % hexane and then centrifuged at 3000 rpm for 3 min to form a pellet. The supernatant was then removed via pipet, and the remaining pellet was immediately redispersed into MeOH via alternating vortexing and sonication for >10 min. Nanoparticle size and dispersity were determined using small-angle X-ray scattering (SAXS) of a capillary filled with a dilute NP in MeOH suspension and was fit using the hard-sphere model (Figure S2). Silicon wafers ((100)) with a thick thermal oxide layer (referred as SiO₂ wafer hereafter) were purchased from Nova Electronic Materials. Silicon wafers ((100)) (Si wafer) were purchased from Wafer World Inc. Higher Mw deuterated polystyrene (dPS, 423 kg/mol, PDI = 1.09) and polystyrene (PS, M_w = 450 kg/mol, PDI = 1.12) were purchased from Polymer Source Inc. Relatively lower M_w dPS (69 kg/mol, PDI = 1.09) was purchased from Polymer Laboratories, and 65 kg/mol (PDI = 1.06) PS was purchased from Pressure Chemical Co. Polymer molecular weights were confirmed via gel permeation chromatography.

Trilayer Fabrication for Nanoparticle Diffusion. We produced trilayer samples with a thin PNC layer between two thick P2VP matrix layers to ensure tracer NP diffusion in our system. This sample

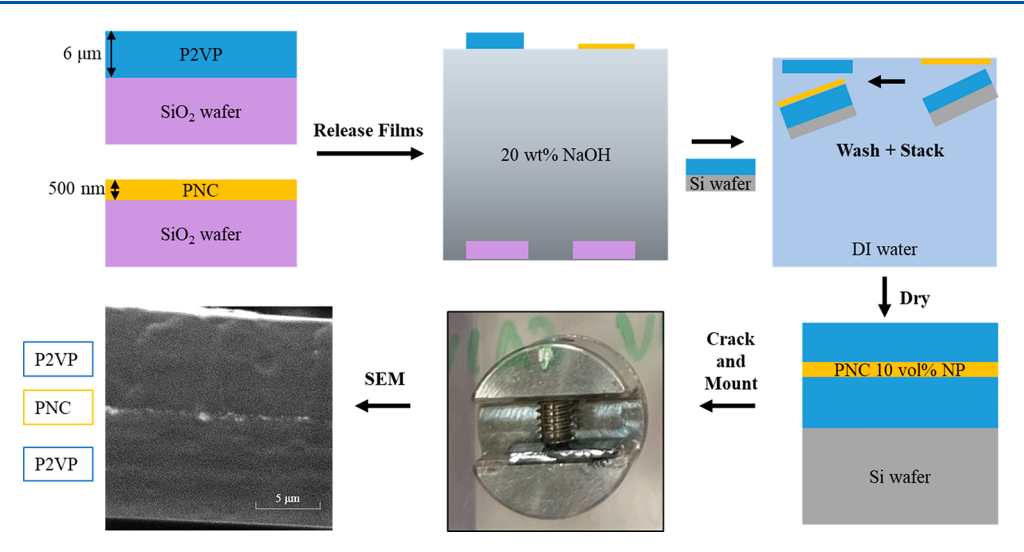


Figure 1. Sample preparation schematic for P2VP-PNC-P2VP trilayers shown in side view. After drying and annealing, the samples were cleaved and mounted for cross-sectional imaging and ToF-SIMS. SEM (30 keV) shows a cross-sectional view of an unannealed 10 vol % NP film between P2VP layers; the free surface of this trilayer sample is visible at the upper right of the image.

geometry permits symmetric diffusion from the nanocomposite into thick P2VP matrix layers, thereby avoiding an influence from the substrate or free surface. This process is summarized in Figure 1. P2VP matrix films ($\sim 6~\mu$ m) were prepared via spin-coating; the P2VP base layer was created by spin-coating 300 g/L P2VP—methanol (MeOH) solutions at 2000 rpm for 1 min onto a silicon (Si) wafer. To prepare the PNC midlayer, 5, 10, or 15 vol % NP in 50 g/L concentration P2VP MeOH solutions were spin-coated onto thermal oxide Si wafers at 2000 rpm for 1 min for a thickness of 500 \pm 60 nm. PNC layers were measured via scanning electron microscopy (SEM), and the thickness was averaged over two samples. The P2VP top layers were spin-coated from 200 g/L P2VP solution onto a thermal oxide treated Si wafer (5 μ m). All solutions were filtered through a 1 μ m mesh filter prior to spin-coating.

To assemble the trilayer samples, the PNC and top P2VP layers on ${\rm SiO_2}$ wafers were gently floated on 20 wt % sodium hydroxide (NaOH)—deionized (DI) water solution until the thin films detached (1.5 h). Using a glass slide, the films were transferred to DI water to remove excess NaOH. A Si wafer with a P2VP bottom layer was slid under the floating film to deposit a PNC layer and then a P2VP top layer. Between deposition samples were briefly dried on a hot plate at 80 °C for 5–10 min to enhance layer adhesion and avoid trapping water between layers. The trilayer samples were then placed in a custom-built oven at 180 °C for 1, 3, or 5 days under vacuum (<50 Pa).

Trilayer Fabrication for Polymer Diffusion. Polymer diffusion trilayers containing a thin dPS midlayer and thick hPS (65 and 450 kg/mol) matrices were fabricated to measure polymer diffusion. The 69K and 423K dPS—toluene solutions (100 and 65 g/L, respectively) were spun-coat at 2000 rpm for 1 min on clean glass slides to produce 400 nm thick midlayers. 65K and 450K PS—toluene solutions (330 and 250 g/L, respectively) were spun-coat at 1000 rpm for 1 min onto an Si wafer for the base layer and onto a clean glass slide for the top layer. The midlayer and top layer of the sample were floated off the glass slides using DI water and stacked onto the base PS layer to create the trilayer sample similar to the process shown in Figure 1.

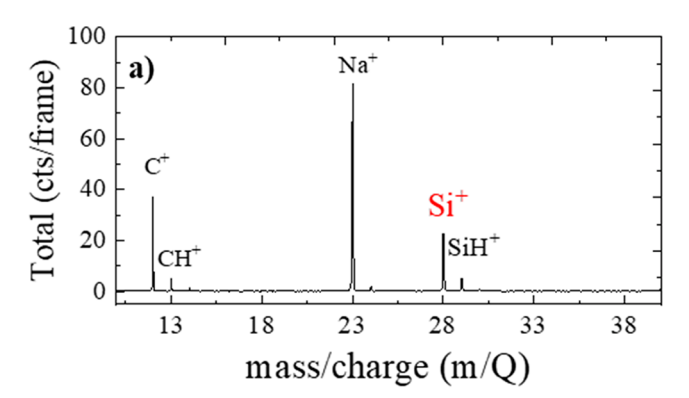
Preparing Trilayer Samples for ToF-SIMS. To obtain the cross-sectional view, a diamond scribe was used to fracture samples along a crystallographic plane of the Si wafer to preserve the polymer/wafer interface and ensure the cross section was as flat as possible. Samples were cleaned with a nitrogen gas gun to remove SiO₂ dust on the surface. To reduce surface charging and improve ion yield, all samples were coated with carbon paint suspended in MEK across the entire back of the wafer and along the front of the polymer film, leaving only ~1 mm of bare polymer and cross-sectional interface. The inset in Figure 3a shows that the Xe⁺ beam is nominally parallel to the

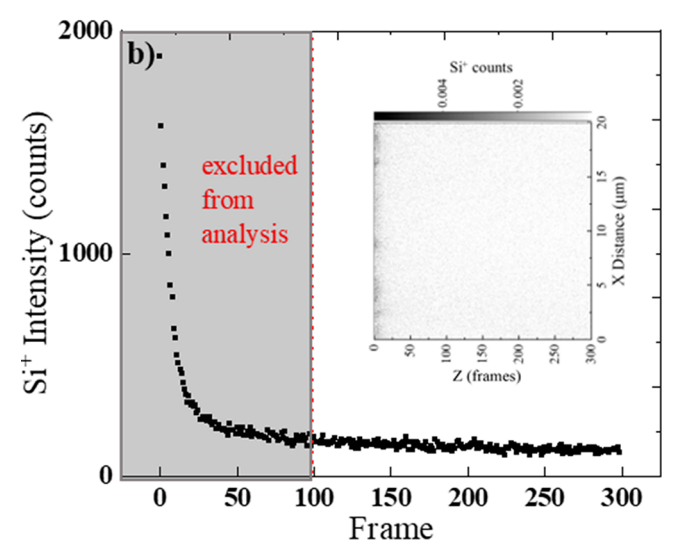
nanocomposite layer and along the Z-axis, so that the composition maps of the X-Y planes will detect the diffusion of nanoparticles into the thick P2VP layers.

ToF-SIMS Method. ToF-SIMS measurements were performed using the Tescan S8252X dual-beam plasma FIB-SEM with Xe+. Unless otherwise noted, measurements were taken with Xe+ FIB parameters at 30 keV and 100 pA with 1024 × 1024 pixel resolution on positive ion mode for 300 frames. A FIB dwell time of 10 μ s and a pulse width of 1000 ns were chosen to measure SiO2 NP diffusion because only a low (m/q < 50) mass range is required, and the pulse width displayed sufficient m/q range. To improve the signal of deuterated PS fragments (C2D2+) using the Xe+ ion beam, polymer diffusion measurements were taken with a pulse width of 3000 ns and for 700 frames. For PNC trilayers, a 20 \times 20 μ m² field of view (FoV) was used, and the ToF-SIMS images were produced using a 2×2 bin width (the minimum required for noise reduction), resulting in an image of 512×512 pixels after processing such that each pixel corresponds to 39 × 39 nm². This pixel size is smaller than the nanoparticle diameter $(2R_{\rm NP})$, ideally permitting single nanoparticle detection. Polymer diffusion measurements were taken with a 15×15 µm FoV to further improve resolution due to the lower intensity signal from the dPS/PS system. While higher pixel resolution is accessible by increasing the pixel count/FoV, it is unnecessary for this experiment and would exponentially increase collection time (Figure S3). Note that our beam conditions prioritize lateral resolution rather than maximizing signal strength because the planar geometry of our trilayer samples allows for us to increase signal by collecting more frames along the z-axis.

■ RESULTS AND DISCUSSION

Measuring NP Concentration Profiles Using ToF-SIMS. In this section we demonstrate our data collection and analysis methods that use ToF-SIMS on a cross-sectional trilayer samples to measure the NP concentration profiles perpendicular to a PNC film. We begin by choosing a defect-free (no cracks, dust, etc.) region of interest (ROI) and establishing that ToF-SIMS detects the PNC layer using a relatively small $20 \times 20~\mu\text{m}^2$ FoV on the trilayer cross section and the silicon secondary ion (Si⁺) (Figure 2a). The mass spectra clearly shows that a FIB dwell time of $10~\mu\text{s}$ and a pulse width of 1000 ns are sufficient to resolve m/q=28 on our instrument. Note that the first 100 frames are omitted due to surface oxidation that distorts the trilayer composition due to the matrix effect previously mentioned (Figure 2b). Removing





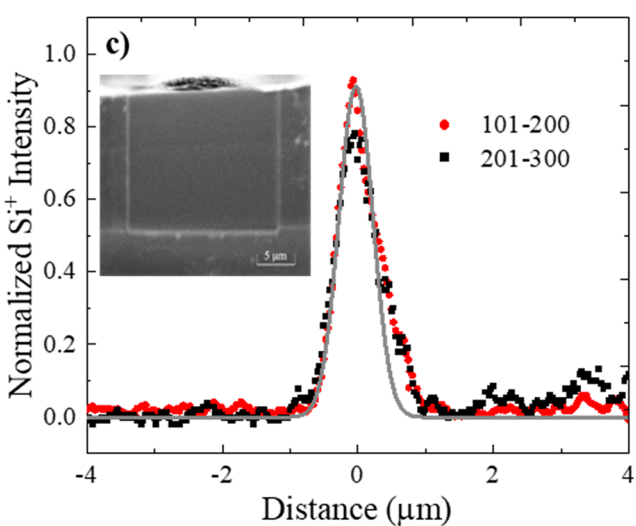
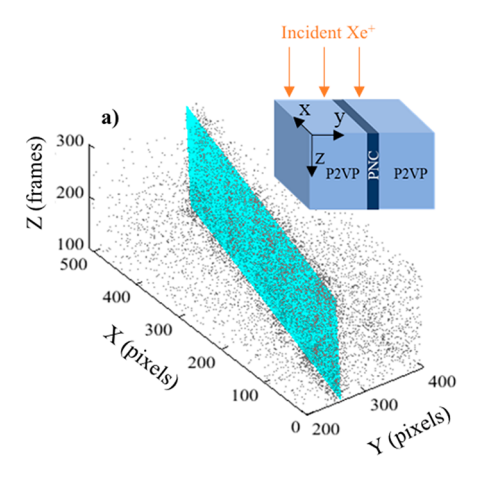


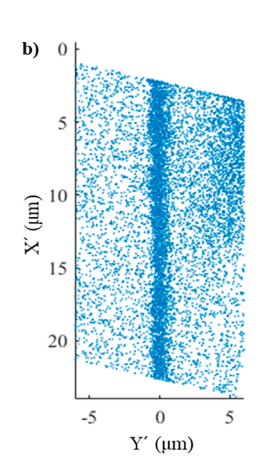
Figure 2. (a) m/Q spectra at 100 pA, 30 keV accelerating voltage for 300 frames for a cross-sectional PNC trilayer sample with 10 vol % NP. Characteristic peak for Si⁺ ion at m/Q = 28. (b) Integrated Si⁺ intensity in the X-Y plane as a function of frame. Inset: projected Si⁺ concentration on the XZ plane displays higher intensity at low frames. (c) Tilt-corrected 1D Si⁺ profile perpendicular to the film fit by convoluting the film profile and the experimental resolution given by a Gaussian FWHM = 0.25 μ m. Data are 3-point averaged (binned). Inset: SEM image of the trilayer cross section after 300 frames displays a flat etched surface. The free surface of the trilayer sample is at the top of the image.

the first 100 frames also eliminates resolution changes due to surface topography, as the sample is smoothed by the FIB. We determined etching rate via atomic force microscopy using a spin-coated PNC film milled under the same conditions as the cross-sectional trilayer sample. We found the etching rate to be ~ 1 nm/frame (Figure S4). These collection parameters result in a total collection time of 52 min per sample, with pixel size and frame count most significantly affecting collection time.

We next determine an experimental resolution function to account for instrumental broadening observed in the concentration profiles. We find the full width at half-maximum (FWHM) of the beam resolution function by modeling the unannealed film as a step function of width 0.5 μ m (as measured by SEM) convoluted with a Gaussian probability density function. By minimizing the residuals between the tiltcorrected 1D concentration profile and the convolution by varying only the FWHM of the Gaussian, we determine the FWHM = 0.25 μ m, which is less than the thickness of the film (Figure 2c). In addition, Figure 2c demonstrates the success of our sample preparation method to create flat trilayer samples for cross-sectional analysis. We confirm that etching rates across the FoV are nonpreferential across the trilayer sample (that is, a flat etching profile is achieved) via SEM, noting there is no significant change in experimental resolution between frames 101-200 and frames 201-300 of data collection. Given that the film is clearly resolved and that its thickness is roughly consistent with SEM measurement (0.5 \pm 0.06 μ m), we demonstrated that ToF-SIMS has sufficient lateral resolution to measure NP diffusion on micrometer length scales as well as sufficient Si⁺ signal from 10 vol % NPs.

We process the 3D compositional maps (Figure 3a) using MATLAB to obtain a 1D concentration profiles for fitting the diffusion coefficients. We detect the SiO₂ NPs in the PNC trilayer samples using frames 101-300 of the Si⁺ ion signal from a 30 keV 100 pA beam current with a spot size of 400 nm. Before extracting 1D concentration profiles perpendicular to the trilayer samples, we rotate the data set and integrate the Si⁺ signal in parallel to the film, which lies approximately in the XZ plane. Rotating the ToF-SIMS data before integrating the intensities in the nominal Z direction is necessary to avoid broadening the Si+ concentration profile. We fit a plane of highest Si⁺ intensity within a ROI determined by a visual inspection of the 3D data where the PNC film should be (pixels 150-450 in Y in this data set) and then define the normal vector to that Si-rich plane. Specifically, we fit the plane using the M-estimator SAmple Consensus (MSAC) algorithm, a variant of the RANdom SAmple Consensus (RANSAC) algorithm, within the MATLAB Computer Vision toolbox to automatically discard background noise from the fitting. 37,38 We select an inlier distance threshold of 25 pixels between the plane and points of consideration to produce a plane fitting and visually inspect for accuracy. After defining the Si-rich plane, we apply the appropriate rotational matrix to orient the film parallel to the Z'-axis and center the film at Y' = 0. Given the 3D nature of ToF-SIMS data, this methodology is required to maximize concentration profile resolution by accounting for sample orientation during sample mounting and data collection. Next, we project the rotated data along the Z'axis (Figure 3b) and integrate along X' to extract a 1D concentration profile. Comparing the raw and rotated profiles in Figure 3c demonstrates that the Si⁺ concentration profile of the unannealed trilayer sample narrows from FWHM = 2.1 to $0.59 \mu m.$





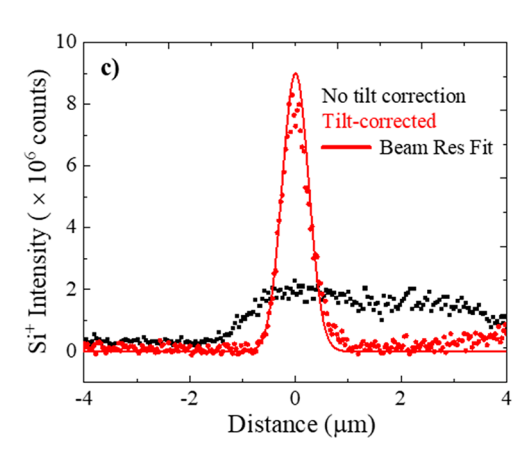


Figure 3. (a) 3D data of Si⁺ density (frames 101–300) of an unannealed trilayer film and the plane fit of maximum Si⁺ density (cyan). (b) X'Y' projection of the Si⁺ density after tilt correction and conversion from pixels to lengths such that Y'=0 intersects with the tilt-corrected plane. (c) 1D profile of Si⁺ intensity across the unannealed trilayer sample integrated before and after tilt correction. Line fit is a convolution of the PNC film thickness (0.5 μ m) and the experimental resolution, FWHM = 0.25 μ m.

Having developed a robust data analysis technique to obtain 1D concentration profiles from ToF-SIMS measurements of trilayer samples, we next optimize the beam conditions for measuring NP diffusion. We choose 30 keV (the maximum) for the accelerating voltage to minimize the spot size and maximize lateral resolution because lateral resolution is the

most important parameter when optimizing measurements of the concentration profile in these cross-sectional trilayer samples. We next determine how beam current impacts the signal-to-background noise ratio on a trilayer sample. By comparing the FWHM of the (tilt-corrected) Si⁺ profiles for 10, 100, and 300 pA Xe⁺ ions, we found a beam current of 100 pA performs with equal resolution to 10 pA, both being superior to 300 pA in these trilayer samples (Figure S5). While a 10 pA beam current has a smaller spot size and higher depth resolution (more frames/nm) compared to the 100 pA current, the Si⁺ signal-to-noise ratio suffers significantly due to low ion extraction counts for equal ToF-SIMS collection duration and does not improve lateral resolution at this length scale. Therefore, 100 pA balances spot size and signal intensity and is the ideal beam current to measure NP diffusion over micrometer length scales.

For comparison, we also investigated a cross section of a PNC trilayer with EDX, finding the line scans to have lower resolution of the Si⁺ signal concentration profile with FWHM = 2.2 μ m. The higher resolution of ToF-SIMS (0.25 μ m) is in part the result of tilt correcting the 3D data. ToF-SIMS provides the unique advantage of direct 3D compositional information from the sample, improving statistics through integrating a 3D data set compared to a 1D EDX line scan. This 3D data also detects local sample inhomogeneity. Relative to EDX, this improves concentration profile quality from ToF-SIMS by allowing the user to mitigate the effect of sample irregularities like sample tilt, surface contamination, or texture during data processing. The close match between FWHM of the EDX film and uncorrected ToF-SIMS data set (2.2 vs 2.1 μ m, respectively) demonstrates that tilt correction is a major contributor to the improved experimental resolution with ToF-SIMS. In addition, the 400 nm collection area of ToF-SIMS is likely smaller than the collection area of EDX, although this was not precisely determined. ToF-SIMS can attain smaller spot sizes, when necessary. In summary, the 3D data and smaller spot size are the most significant advantages of ToF-SIMS over EDX for measuring NP concentration profiles. Also, unlike EDX ToF-SIMS detects various polymer fragments to measure polymer concentration profiles and thus polymer diffusion, as demonstrated below.

Tracer Diffusion Coefficients of NPs in Polymer. The tilt-corrected 1D Si⁺ concentration profiles were used to determine the tracer diffusion coefficient of silica NPs sandwiched between two polymer matrix films. We analyzed trilayer samples annealed at 180 °C for 1, 3, and 5 days with 10 vol % NPs using aforementioned beam conditions (Figure 4). First, we deconvoluted the instrumental beam resolution function from the tilt-corrected 1D Si⁺ profile to obtain the NP concentration profile. Then, we iteratively fit the solution of Fick's second law for a finite source diffusing into a semi-infinite medium to the concentration profiles.

$$\varphi(y) = \frac{1}{2} \left[\operatorname{erf} \left(\frac{h - y}{\sqrt{4D_{\text{NP}}t}} \right) + \operatorname{erf} \left(\frac{h + y}{\sqrt{4D_{\text{NP}}t}} \right) \right] \tag{1}$$

where $\varphi(y)$ is the concentration as a function of position y,h indicates the film's initial thickness ($h=0.50~\mu\mathrm{m}$), D_{NP} is the NP diffusion coefficient, and t is time in seconds. The fits resulted in D_{NP} of 2.2×10^{-14} , 1.9×10^{-14} , and 2.5×10^{-14} cm²/s respectively for the 1, 3, and 5 day anneals. Averaging over all three samples yields $D_{\mathrm{NP}}=2.3\times10^{-14}~\mathrm{cm}^2/\mathrm{s}$, with NPs traveling \sim 1.9 $\mu\mathrm{m}$ at 5 days $x\sim2(Dt)^{0.5}$. A standard

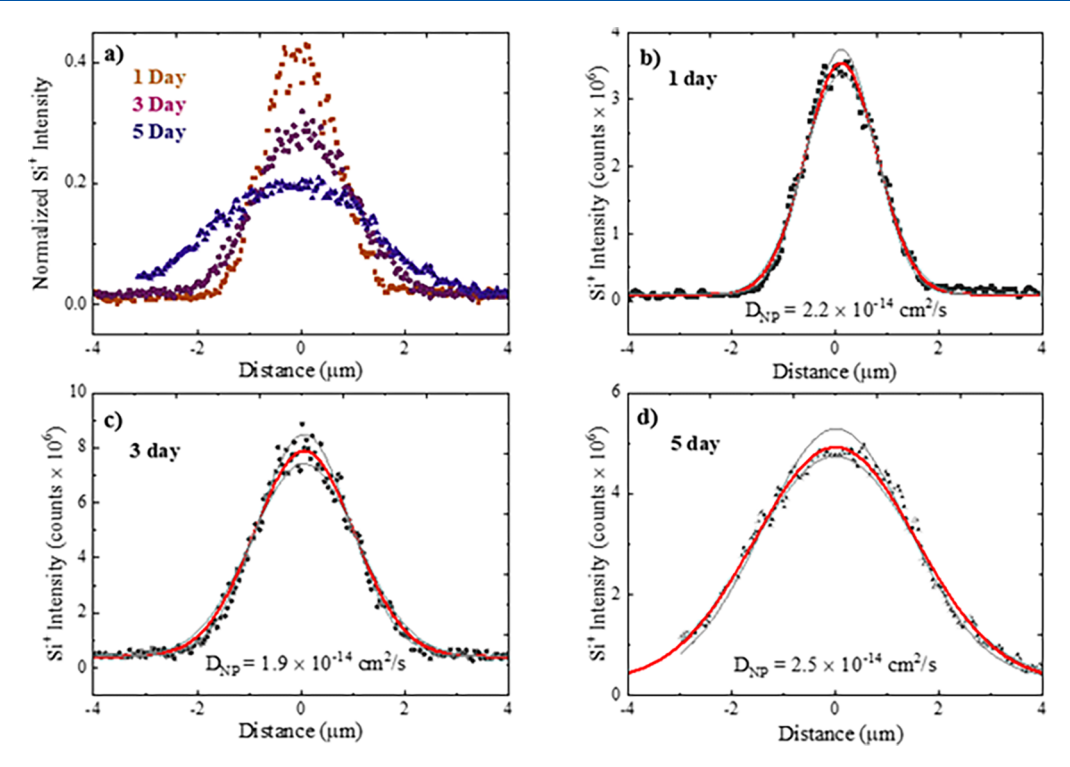
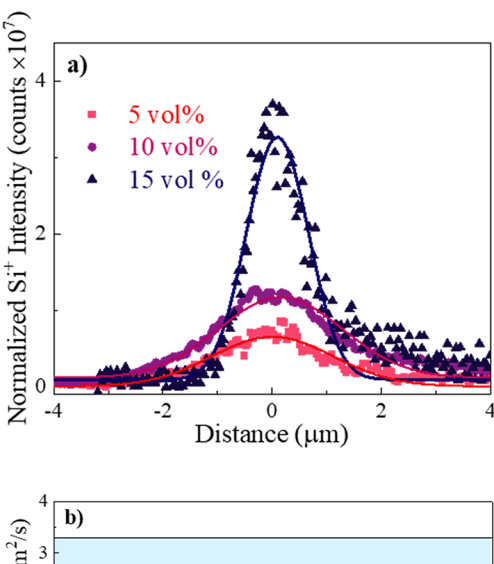


Figure 4. Si⁺ concentration profiles are fit with eq 1 as described in the text to find the NP tracer diffusion coefficient $D_{\rm NP}$. Fits for $D_{\rm NP} \pm \delta$ are shown in gray; the best fit is shown in red. (a) The Si⁺ profiles for all annealed samples. $D_{\rm NP}$'s from samples annealed at 180 °C for (b) 1 day, (c) 3 days, and (d) 5 days show excellent agreement.

deviation of 0.4 \times 10⁻¹⁴ cm²/s across three samples shows good consistency as a function of annealing time, indicating a single-mode NP diffusion. Deviating the best $D_{\rm NP}$ by a factor δ = 0.3 \times 10⁻¹⁴ cm²/s results in a significant decrease in R^2 (Table S1) and visually worse goodness-of-fit (Figure 4), confirming the reliability of our fitting procedure.

Our NP diffusion coefficient is in excellent agreement with an earlier study that used RBS.¹⁷ There, Griffin et al. determined $D_{\rm NP}$ for silica NPs with $R_{\rm NP}$ = 13 nm in a 100 kg/mol P2VP system at T = 180 °C. We linearly extrapolate their result using the Stokes-Einstein model to estimate $D_{\rm NP}$ for our experiment ($R_{\rm NP}$ = 26.1 nm, 100 kg/mol P2VP, 180 °C): $D_{\rm NP-est}$ = (1.9–3.3) × 10⁻¹⁴ cm²/s. The range is due to estimations of the true volume fraction of NP during annealing;¹⁷ see the Supporting Information for additional details. Our ToF-SIMS results are in excellent agreement with the D_{NP-est} . Notably, the RBS measurements were performed in a bilayer sample on the length scale of <500 nm, leading to diffusion time scales limited to ~30 min. These ToF-SIMS measurements capture diffusion distances of several μ m and allow for a wider range of diffusion times and speeds, in particular for faster diffusing species that require this extended accessible length scale.

Finally, we note that tracer diffusion experiments require low NP concentrations, so that $D_{\rm NP}$ is independent of NP concentration. While using the experimental and analysis protocols established above, we measure $D_{\rm NP}$ after a 3 day anneal at 180 °C using PNC layers with 5 and 15 vol % (Figure 5). As expected, the 5 vol % sample displays a decrease in the Si⁺ intensity compared to background; therefore, 600 frames were collected to improve signal while maintaining the same beam resolution. Collecting additional frames would produce better signal-to-noise statistics at all loadings but is only necessary for lower particle loadings. The $D_{\rm NP}$ values



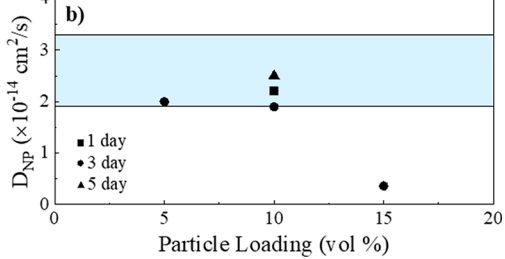
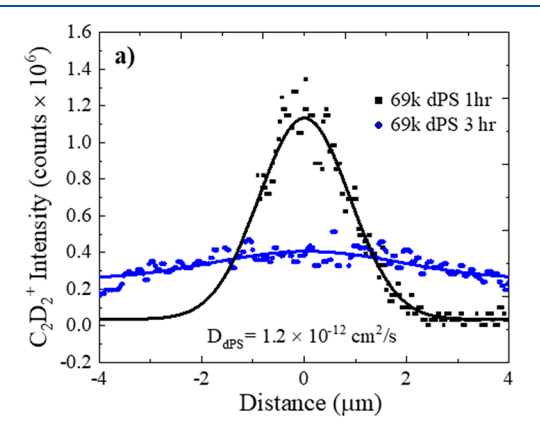


Figure 5. (a) Diffusion profiles of 5 vol % (squares, 101–600 frames), 10 vol % (circles, 101–300 frames), and 15 vol % (triangles, 101–300 frames) NPs annealed for 3 days at 180 °C. (b) $D_{\rm NP}$ as a function of NP loading and at 10 vol % as a function of annealing time. Shaded area (blue) shows an estimate based on previous work using RBS to measure NP tracer diffusion.

determined for 5 and 10 vol % are 2.0×10^{-14} and 1.9×10^{-14} cm²/s, respectively, and in excellent agreement with one another and with ERD values. Comparatively, raising the particle loading to 15% results in a substantially lower the diffusion coefficient, $D_{\rm NP} = 0.36 \times 10^{-14}$ cm²/s. By this study of NP loading, we determine that 15 vol % is above the tracer diffusion regime. Goodness-of-fit (R^2) results for each sample are provided in Table S1.

Polymer Tracer Diffusion Coefficients. We modified our ToF-SIMS methodology for measuring NP concentration profiles to measure polymer concentration profiles by adjusting a few instrument parameters to improve signal. Applying ToF-SIMS to trilayers of polystyrene/deuterated polystyrene/polystyrene, we measure the $C_2D_2^+$ (m/q=28) concentration profiles and compute the dPS tracer diffusion coefficients. Both $C_2D_2^+$ and Si⁺ ions have m/q=28, so we used the C⁺ (m/q=12) signal to confirm the location of the deuterated polymer layer within the trilayer sample (Figure S6). After tilt correction of the ToF-SIMS data, the 1D $C_2D_2^+$ profiles were deconvoluted from the experimental resolution function and fit to eq 1 (Figure 6). For the 65K–69K hPS/dPS system,



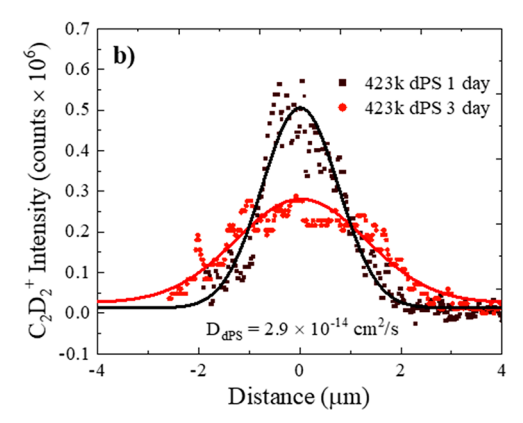


Figure 6. $C_2D_2^+$ concentration profiles are fit with eq 1 to find the dPS tracer diffusion coefficient $D_{\rm dPS}$. Trilayers were annealed at 174 °C for (a) 69K–65K dPS/PS for 1 and 3 h and (b) 423K–450K dPS/PS for 1 and 3 days. Data are binned for noise reduction.

annealed for 1 and 3 h at 174 °C, the $D_{\rm dPS}$ values are 1.0 × 10^{-12} and 1.3 × 10^{-12} cm²/s. The $D_{\rm dPS}$ values are 2.8 × 10^{-14} and 3.0 × 10^{-14} cm²/s for the 450K–423K hPS/dPS system annealed at 174 °C for 1 and 3 days, respectively. Excellent agreement was found for both molecular weights as a function of annealing time. The goodness-of-fit (R^2) for each sample is provided in Table S3.

Polystyrene tracer diffusion was previously measured using ERD by Green et al., where a 10-20 nm deuterated PS layer diffused into a $\sim 4~\mu m$ PS $(M_{\rm w}=2\times10^7)$ bottom layer upon annealing at 174 $^{\circ}{\rm C.^{27}}$ In the limit of high PS molecular weight, the tracer diffusion coefficient was found to depend on the dPS molecular weight as $D_{\rm PS}=0.008{\rm M^{-2}}$ (Figure S7). Applying this result to our molecular weights gives $D_{\rm Green(69K)}=1.7\times10^{-12}~{\rm cm^2/s}$ and $D_{\rm Green(423K)}=4.0\times10^{-14}~{\rm cm^2/s}$. Our results with ToF-SIMS are in excellent agreement with these earlier results using ERD, further demonstrating the value of ToF-SIMS for measuring diffusion coefficients in polymer systems.

Future Potential of ToF-SIMS for Measuring Diffusion **Coefficients.** While we demonstrated the ability of ToF-SIMS to measure NP and polymer tracer diffusion coefficients on a large length scale ($\sim 2 \mu m$), a key advantage of ToF-SIMS is its ability to vary resolution to access a variety of length scales. Specifically, diffusion lengths across an exceptionally large range (0.3–100s μ m) can be accommodated by selecting appropriate FoV and pixel count settings.^{39,40} Beam current, accelerating voltage, and frame count can likewise be adjusted to improve intensity or lateral resolution as needed. Therefore, in any PNC or polymer melt trilayer sample with a diffusing layer that can be identified by a contrasting m/q value, a diffusion coefficient can be determined. To estimate the accessible diffusion coefficients, we use $x = 2\sqrt{Dt}$, where D is the diffusion coefficient, t is the diffusing time in seconds, and x is the distance diffused. Assuming a minimum practical spot size of 200 nm for our Xe+ ToF-SIMS instrument and convenient annealing times from 10 min to 7 days, ToF-SIMS can measure diffusion coefficients from 10^{-15} to 10^{-6} cm²/s (Figure 7). In this paper, we have demonstrated a range of diffusion coefficients from 10^{-15} to 10^{-12} cm²/s as noted by the symbols in Figure 7.

Ideal systems for Xe⁺ ToF-SIMS contain polar components such as oxide-based particles that take advantage of the matrix effect or low mass fragments (m < 50).³¹ These factors are important when choosing a PNC system to maximize signal in a primary ion beam system. Cluster ion beams are preferred for polymer systems for their ability to identify larger organic

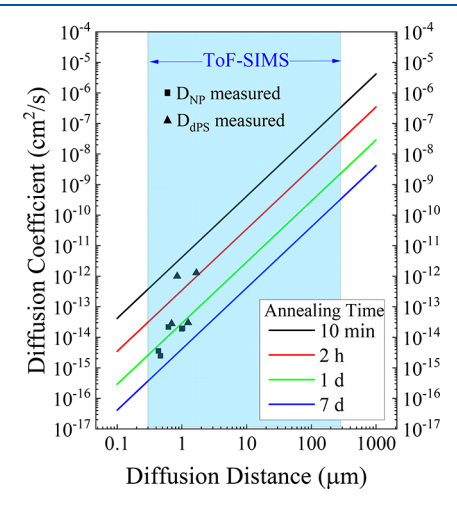


Figure 7. Diffusion coefficient $(D = x^2/4t)$ as a function of diffusion distance (x) for a range of annealing times (10 min to 7 days). ToF-SIMS can measure concentration profiles with resolutions from 0.3 to $\sim 200 \ \mu \text{m}$ indicating the ability to measure diffusion coefficients from 10^{-15} to 10^{-6} cm²/s (blue).

fragments as the diffusing species. Crowded NP systems, which are commercially more important and can be analogues to biological systems, can be investigated with no upper limit on particle loading. Conversely, very dilute NP systems, as necessary to avoid NP aggregation, can likewise be investigated with ToF-SIMS by compensating with higher frame counts. Furthermore, ToF-SIMS uniquely provides a 3D compositional profile of the sample, allowing for imperfections like surface roughness or sample blemishes to be excluded from the diffusion profile. With a cryo-stage attachment, ToF-SIMS can also be used to probe materials that are a melt at room temperature ($T_{\rm g} < T_{\rm room}$). While our ToF-SIMS method using cross-sectional trilayers has been demonstrated for two specific cases of NP and polystyrene diffusion, the future opportunities abound.

CONCLUSIONS

We demonstrate a versatile ToF-SIMS method to measure diffusion coefficients using a trilayer sample geometry and a cross-sectional measurement by optimizing sample preparation, ToF-SIMS parameters, and data processing. An accelerating voltage of 30 keV is most appropriate to maximize lateral resolution in our Xe+ ToF-SIMS. The beam current impacts lateral resolution and depth resolution, and 100 pA performs best for our materials with a lateral spot size of <0.5 μ m and an etching rate of \sim 1 nm/frame. We use an image size of 1024 × 1024 pixel resolution (prebinning) which balances collection times (typically ~1 h) and lateral resolution to give a pixel size smaller than the NP diameter. This pixel size is also sufficiently smaller than the spot size of the ion beam (spot size $\gg 2 \times \text{pixel size}$) to ensure the entire pixel area is milled per frame, and a 2×2 bin is applied to the image to reduce noise. A dwell time of 10 μs is sufficient to resolve the Si⁺ ion in our PNC system, the significant species for identifying NP location, and to resolve C₂D₂⁺ in our dPS/PS system. We also established a protocol for rotating and centering the 3D composition data prior to integrating to a 1D concentration profile perpendicular to the trilayer sample.

We demonstrate the accuracy of measuring diffusion coefficients of nanoparticles and polymers using ToF-SIMS by comparing to previous studies. Excellent agreement was found for $D_{\rm NP}$ of silica NPs in P2VP and for $D_{\rm dPS}$ in polystyrene at two molecular weights. In addition, we establish that in a 10 vol % NP trilayer, $D_{\rm NP}$ is independent of annealing time (1–5 days) and that with a 3 day anneal $D_{\rm NP}$ is independent of NP vol % when <10 vol %.

This ToF-SIMS methodology has great potential for investigating unexplored PNCs across a wide range of chemistries, lateral resolutions, length scales, and concentrations, thus expanding the understanding of NP diffusion in polymer melts. ToF-SIMS can likewise expand polymer—polymer diffusion in miscible polymer system with or without the use of deuterated polymers, if there are unique polymer fragments for the two polymers. ToF-SIMS can reinvigorate diffusion studies vital to open polymer physics questions and interesting PNC systems.

ASSOCIATED CONTENT

Supporting Information

The Supporting Information is available free of charge at https://pubs.acs.org/doi/10.1021/acs.macromol.3c00033.

Figure S1: SANS characterization of polymer $R_{\rm g}$; Figure S2: SAXS characterization of NP size and distribution; Figure S3: pixel resolution and collection time comparison; Figure S4: AFM image and traces of 300 frame ToF-SIMS PNC; Figure S5: 1D Si⁺ concentration profiles at 10 and 100 pA; Table S1: R^2 goodness-of-fit values for Figure 4; $D_{\rm NP}$ for comparison: details of the calculation of expected $D_{\rm NP}$ values based on literature; Table S2: effective volume percent, effective viscosity, and respective $D_{\rm NP}$ range based on literature; Figure S6: 2D compositional maps of deuterated PS; Table S3: R^2 goodness of fit values for Figure 6; Figure S7: $D_{\rm dPS}$ for comparison with details of previous experimental and theoretical values (PDF)

AUTHOR INFORMATION

Corresponding Author

Karen I. Winey — Department of Materials Science and Engineering and Department of Chemical and Biomolecular Engineering, Department of Materials Science and Engineering, University of Pennsylvania, Philadelphia, Pennsylvania 19104, United States; ○ orcid.org/0000-0001-5856-3410; Email: winey@seas.upenn.edu

Authors

Kaitlin Wang — Department of Materials Science and Engineering, University of Pennsylvania, Philadelphia, Pennsylvania 19104, United States; orcid.org/0000-0003-2459-8767

Russell J. Composto – Department of Materials Science and Engineering, University of Pennsylvania, Philadelphia, Pennsylvania 19104, United States; orcid.org/0000-0002-5906-2594

Complete contact information is available at: https://pubs.acs.org/10.1021/acs.macromol.3c00033

Notes

The authors declare no competing financial interest.

ACKNOWLEDGMENTS

We acknowledge funding from DOE BES DE-SC0016421 and ExxonMobil Research and Engineering (K.W., K.I.W.). We thank Dr. Jamie Ford at the Singh Center for Nanotechnology at the University of Pennsylvania for expertise regarding ToF-SIMS, supported by NSF-MRSEC-DMR-1720530. We also thank Peter Beaucage at NIST for providing SANS work to determine polymer $R_{\rm g}$. Support was also provided by NSF-POLYMERS DMR 1905912 (R.J.C.), NSF-MRSEC-DMR 1720530 (R.J.C.), and NSF-CBET- 2034122 (K.I.W., R.J.C.). We also acknowledge funding from NSF-NRT-2152205 (K.W., R.J.C., K.I.W.).

REFERENCES

- (1) Kumar, S. K.; Benicewicz, B. C.; Vaia, R. A.; Winey, K. I. 50th Anniversary Perspective: Are Polymer Nanocomposites Practical for Applications? *Macromolecules* **2017**, *50*, 714–731.
- (2) Bailey, E. J.; Winey, K. I. Dynamics of Polymer Segments, Polymer Chains, and Nanoparticles in Polymer Nanocomposite Melts: A Review. *Prog. Polym. Sci.* **2020**, *105*, 101242.
- (3) Thakur, V. K.; Kessler, M. R. Self-Healing Polymer Nanocomposite Materials: A Review. Polymer (Guildf) 2015, 69, 369–383.

- (4) Balazs, A. C.; Emrick, T.; Russell, T. P. Nanoparticle Polymer Composites: Where Two Small Worlds Meet. *Science* (80-.) **2006**, 314, 1107–1110.
- (5) Raemdonck, K.; Braeckmans, K.; Demeester, J.; De Smedt, S. C. Merging the Best of Both Worlds: Hybrid Lipid-Enveloped Matrix Nanocomposites in Drug Delivery. *Chem. Soc. Rev.* **2014**, *43*, 444.
- (6) Mills, P. J.; Green, P. F.; Palmstrøm, C. J.; Mayer, J. W.; Kramer, E. J. Polydispersity Effects on Diffusion in Polymers: Concentration Profiles of d-Polystyrene Measured by Forward Recoil Spectrometry. J. Polym. Sci., Part B: Polym. Phys. 1986, 24, 1–9.
- (7) Green, P. F.; Kramer, E. J. Matrix Effects on the Diffusion of Long Polymer Chains. *Macromolecules* **1986**, *19*, 1108–1114.
- (8) Mackay, M. E.; Dao, T. T.; Tuteja, A.; Ho, D. L.; van Horn, B.; Kim, H.-C.; Hawker, C. J. Nanoscale Effects Leading to Non-Einsteinlike Decrease in Viscosity. *Nat. Mater.* 2003, 2, 762–766.
- (9) Composto, R. J.; Mayer, J. W.; Kramer, E. J.; White, D. M. Fast Mutual Diffusion in Polymer Blends. *Phys. Rev. Lett.* **1986**, *57*, 1312–1315.
- (10) Composto, R. J.; Kramer, E. J.; White, D. M. Mutual Diffusion in the Miscible Polymer Blend Polystyrene/Poly(Xylenyl Ether). *Macromolecules* **1988**, *21*, 2580–2588.
- (11) Barrat, J.-L.; Fredrickson, G. H. Diffusion of a Symmetric Block Copolymer in a Periodic Potential. *Macromolecules* **1991**, *24*, 6378–6383
- (12) Gam, S.; Meth, J. S.; Zane, S. G.; Chi, C.; Wood, B. A.; Seitz, M. E.; Winey, K. I.; Clarke, N.; Composto, R. J. Macromolecular Diffusion in a Crowded Polymer Nanocomposite. *Macromolecules* **2011**, *44*, 3494–3501.
- (13) Lin, C. C.; Parrish, E.; Composto, R. J. Macromolecule and Particle Dynamics in Confined Media. *Macromolecules* **2016**, 49, 5755–5772.
- (14) Tuteja, A.; Mackay, M. E.; Narayanan, S.; Asokan, S.; Wong, M. S. Breakdown of the Continuum Stokes-Einstein Relation for Nanoparticle Diffusion. *Nano Lett.* **2007**, *7*, 1276–1281.
- (15) Carroll, B.; Bocharova, V.; Carrillo, J.-M. Y.; Kisliuk, A.; Cheng, S.; Yamamoto, U.; Schweizer, K. S.; Sumpter, B. G.; Sokolov, A. P. Diffusion of Sticky Nanoparticles in a Polymer Melt: Crossover from Suppressed to Enhanced Transport. *Macromolecules* **2018**, *51*, 2268–2275.
- (16) Park, J.; Bailey, E. J.; Composto, R. J.; Winey, K. I. Single-Particle Tracking of Nonsticky and Sticky Nanoparticles in Polymer Melts. *Macromolecules* **2020**, *53*, 3933–3939.
- (17) Griffin, P. J.; Bocharova, V.; Middleton, L. R.; Composto, R. J.; Clarke, N.; Schweizer, K. S.; Winey, K. I. Influence of the Bound Polymer Layer on Nanoparticle Diffusion in Polymer Melts. *ACS Macro Lett.* **2016**, *5*, 1141–1145.
- (18) Cole, D. H.; Shull, K. R.; Rehn, L. E.; Baldo, P. M. RBS Analysis of the Diffusion of Nano-Size Spheres in a Polymer Matrix. *Nucl. Instruments Methods Phys. Res. Sect. B Beam Interact. with Mater. Atoms* 1998, 136–138, 283–289.
- (19) Parrish, E.; Caporizzo, M. A.; Composto, R. J. Network Confinement and Heterogeneity Slows Nanoparticle Diffusion in Polymer Gels. *J. Chem. Phys.* **2017**, *146*, 203318.
- (20) Shrestha, U. M.; Han, L.; Saito, T.; Schweizer, K. S.; Dadmun, M. D. Mechanism of Soft Nanoparticle Diffusion in Entangled Polymer Melts. *Macromolecules* **2020**, *53*, 7580–7589.
- (21) Imel, A. E.; Rostom, S.; Holley, W.; Baskaran, D.; Mays, J. W.; Dadmun, M. D. The Tracer Diffusion Coefficient of Soft Nanoparticles in a Linear Polymer Matrix. *RSC Adv.* **2017**, *7*, 15574–15581.
- (22) Jo, K. Il; Oh, Y.; Kim, T. H.; Bang, J.; Yuan, G.; Satija, S. K.; Sung, B. J.; Koo, J. Position-Dependent Diffusion Dynamics of Entangled Polymer Melts Nanoconfined by Parallel Immiscible Polymer Films. ACS Macro Lett. 2020, 9, 1483–1488.
- (23) Green, P. F.; Palmstrom, C. J.; Mayer, J. W.; Kramer, E. J. Marker Displacement Measurements of Polymer-Polymer Interdiffusiont. *Macromolecules* **1985**, *18*, 501–507.

- (24) Jimenez, A. M.; Zhao, D.; Misquitta, K.; Jestin, J.; Kumar, S. K. Exchange Lifetimes of the Bound Polymer Layer on Silica Nanoparticles. *ACS Macro Lett.* **2019**, *8*, 166–171.
- (25) Lin, C.-C.; Griffin, P. J.; Chao, H.; Hore, M. J. A.; Ohno, K.; Clarke, N.; Riggleman, R. A.; Winey, K. I.; Composto, R. J. Grafted Polymer Chains Suppress Nanoparticle Diffusion in Athermal Polymer Melts. J. Chem. Phys. 2017, 146, 203332.
- (26) Composto, R. J.; Kramer, E. J. Mutual Diffusion Studies of Polystyrene and Poly(Xylenyl Ether) Using Rutherford Backscattering Spectrometry. *J. Mater. Sci.* **1991**, *26*, 2815–2822.
- (27) Mills, P. J.; Green, P. F.; Palmstrom, C. J.; Mayer, J. W.; Kramer, E. J. Analysis of Diffusion in Polymers by Forward Recoil Spectrometry. *Appl. Phys. Lett.* **1984**, 45, 957.
- (28) Martin, J.; Hernández-Vélez, M.; de Abril, O.; Luna, C.; Munoz-Martin, A.; Vázquez, M.; Mijangos, C. Fabrication and Characterization of Polymer-Based Magnetic Composite Nanotubes and Nanorods. *Eur. Polym. J.* **2012**, *48*, 712–719.
- (29) Bailey, E. J.; Griffin, P. J.; Composto, R. J.; Winey, K. I. Characterizing the Areal Density and Desorption Kinetics of Physically Adsorbed Polymer in Polymer Nanocomposite Melts. *Macromolecules* **2020**, *53*, 2744–2753.
- (30) Composto, R. J.; Walters, R. M.; Genzer, J. Application of Ion Scattering Techniques to Characterize Polymer Surfaces and Interfaces. *Mater. Sci. Eng. R Reports* **2002**, *38*, 107–180.
- (31) Spool, A. M. The Practice of TOF-SIMS: Time of Flight Secondary Ion Mass Spectrometry Alan M. Spool Google Books; Momentum Press: 2016.
- (32) Mei, H.; Laws, T. S.; Terlier, T.; Verduzco, R.; Stein, G. E. Characterization of Polymeric Surfaces and Interfaces Using Time-of-Flight Secondary Ion Mass Spectrometry. *J. Polym. Sci.*; John Wiley and Sons Inc.: April 1, 2021; pp 1174–1198.
- (33) Prasad, A.; Salim, N. V.; Mozetič, M.; Kailas, L.; Thomas, S. Time-of-Flight Secondary Ion Mass Spectrometric Analysis of Polymer Surfaces: A Review. *J. Appl. Polym. Sci.* **2022**, 139, 52286.
- (34) Bailey, J.; Havelund, R.; Shard, A. G.; Gilmore, I. S.; Alexander, M. R.; Sharp, J. S.; Scurr, D. J. 3D ToF-SIMS Imaging of Polymer Multilayer Films Using Argon Cluster Sputter Depth Profiling. ACS Appl. Mater. Interfaces 2015, 7, 2654–2659.
- (35) Sui, T.; Song, B.; Dluhos, J.; Lu, L.; Korsunsky, A. M. Nanoscale Chemical Mapping of Li-Ion Battery Cathode Material by {FIB-SEM} and {TOF-SIMS} Multi-Modal Microscopy. *Nano Energy* **2015**, *17*, 254–260.
- (36) Karar, N.; Gupta, T. K. Study of Polymers and Their Blends Using TOF-SIMS Ion Imaging. *Vacuum* **2015**, *111*, 119–123.
- (37) Fit plane to 3-D point cloud MATLAB pcfitplane; https://www.mathworks.com/help/vision/ref/pcfitplane.html (accessed 2022-06-22).
- (38) Fischler, M. A.; Bolles, R. C. Random Sample Consensus. *Commun. ACM* **1981**, *24*, 381–395.
- (39) Richardin, P.; Mazel, V.; Walter, P.; Laprévote, O.; Brunelle, A. Identification of Different Copper Green Pigments in Renaissance Paintings by Cluster-TOF-SIMS Imaging Analysis. *J. Am. Soc. Mass Spectrom.* **2011**, *22*, 1729–1736.
- (40) Belu, A. M.; Davies, M. C.; Newton, J. M.; Patel, N. TOF-SIMS Characterization and Imaging of Controlled-Release Drug Delivery Systems. *Anal. Chem.* **2000**, *72*, 5625–5638.